Estimation of J-integral for a Non-local Particle Model Using Atomistic Finite Element Method and Coupling Between Non-local Particle and Finite Element Methods

by

Jayesh Zope

A Thesis Presented in Partial Fulfillment
of the Requirements for the Degree
Master of Science

Approved July 2016 by the
Graduate Supervisory Committee:

Yongming Liu, Chair
Jay Oswald
Hanqing Jiang

ARIZONA STATE UNIVERSITY

August 2016

ABSTRACT

In this paper, at first, analytical formulation of J-integral for a non-local particle model (VCPM) using atomic scale finite element method is proposed for fracture analysis of 2D solids. A brief review of classical continuum-based J-integral and a non-local lattice particle method is given first. Following this, detailed derivation for the J-integral in discrete particle system is given using the energy equivalence and stress-tensor mapping between the continuum mechanics and lattice-particle system. With the help of atomistic finite element method, the J-integral is expressed as a summation of the corresponding terms in the particle system.

Secondly, a coupling algorithm between a non-local particle method (VCPM) and the classical finite element method (FEM) is discussed to gain the advantages of both methods for fracture analysis in large structures. In this algorithm, the discrete VCPM particle and the continuum FEM domains are solved within a unified theoretical framework. A transitional element technology is developed to smoothly link the 10-particles element with the traditional FEM elements to guaranty the continuity and consistency at the coupling interface. An explicit algorithm for static simulation is developed.

Finally, numerical examples are illustrated for the accuracy, convergence, and path-independence of the derived J-integral formulation. Discussions on the comparison with alternative estimation methods and potential application for fracture simulation are given. The accuracy and efficiency of the coupling algorithm are tested by several benchmark problems such as static crack simulation.

ACKNOWLEDGMENTS

I would like to thank Prof. Yongming Liu, whose expertise, understandings, generous guidance and support made it possible for me to work on a topic that was of great interest to me. It was a pleasure working with him.

My sincere thanks also goes to the members of my graduate committee, Prof. Jay Oswald and Prof. Hanqing Jiang for their patience and understanding during a year of effort that went into the production of this research.

A special thanks also to Prof. Enqiang Lin, from whose paper many of the concepts used in this research paper have been quoted. Another special thanks to Dr. Hailong Chen who provided the previous materials and links upon which much of this is based and for help with timely reply to my emails.

TABLE OF CONTENTS

LIST OF TABLES

LIST OF FIGURES

Figure Page

Chapter 1

INTRODUCTION

The J-integral formulation for 2D solid was introduced by Rice (Rice 1968). The J-integral value was shown to be path independent and equivalent with the energy release rate. The J-integral can be understood both as a fracture energy parameter and as a stress intensity parameter because J uniquely characterizes crack-tip stresses and strains. The J-integral has been extensively used to compute energy flow near the crack tip, to estimate crack opening displacement, and to formulate various fracture criteria for engineering materials. Numerous analytical and numerical studies have been done for the estimation and application of J-integral for continuum-based fracture analysis and will not be further discussed here as it is not the intent of this paper. The main objective of the proposed study is to develop an estimation method for J-integral based on the discrete representation of solids with cracks. Thus, correspondence of fracture analysis using continuum-based and discrete formulation can be established.

There are essentially two major approaches for fracture analysis of solids: continuum-based and discrete approach. One widely used discrete approach for fracture simulation is the molecular dynamics (Holian and Ravelo 1995). Lattice particle method or spring network method is another major type of discrete approach and have been extensively investigated (Zhao, Fang, and Zhao 2011). All these model differs in the fundamental hypotheses, formulation, and solution algorithms, but can be grouped in two major categories: local approach and non-local approach. For local approach, interactions between particles/nodes/joints only depends on the neighboring local particles/nodes/joints. The local interactions can be uniaxial or can

be multiaxial. For non-local approach, interactions between particles not only depends on the neighboring local particles, but also have contributions from the surrounding non-local particles/nodes/joints proposed by Chen (Chen, Lin, and Liu 2014). The non-local approach has been shown to be flexible to model various solid fracture problems and will be the focus of this study.

Many numerical models have been proposed to overcome these difficulties, such as the particle method (Hrennikoff 1941; Ostoja-Starzewski 2002; Noor 1988). Particle-based models represent materials by a system of particles and simulate the underlying physics on the level of micro-mechanical interaction rules among those particles. The basic idea is very similar to the idea behind the molecular dynamics. The governing law of the dynamics of particles is Newton's equations of motion. These equations are usually discretized in time and do not involve spatial derivatives that require the hypothesis of continuity of the material. Thus, particle-based methods are discontinuous formulation of solids which are especially suitable for simulation of crack growth, deflection and branching problems.

A novel volumetric-compensated particle model (VCPM) (Chen, Lin, and Liu 2014) has been recently proposed to further improve the Poisson ratio's restriction by introducing a non-local multi-body particle interaction into the conventional lattice model. This is done by treating the solid as a collection of regularly distributed deformable particles that inter-connected each other by a network of normal springs. The novelty of the VCPM lies in two aspects: (1) the particles are treated as deformable bodies which can store volumetric strain energies; and (2) the corresponding non-local multi-body particle interactions caused by the particles' volume change effects are included only through the pair-wise normal spring interactions, which greatly facilitates the computation. One of the most important benefits of the particle-based

simulation is that it can describe the fracture of materials by directly incorporating a cohesive type law into the particle interactions, like the virtual internal bond (VIB) model proposed by Gao (Gao and Klein 1998).

Most fracture analysis using discrete approach focuses on the simulation with microscopic damage rules of spring/bonds. Relatively few studies try to calculate the driving force parameters in the classical fracture mechanics using the discrete methods. Jin and Yuan (Jin and Yuan 2005) established the connections of fracture parameters between microscopic and macroscopic description of fracture by using molecular mechanics simulation to calculate the energy release rates and stress fields in covalently bonded solids under small strain deformation. Alternative approaches for atomistic J-integral (Zimmerman and Jones 2013; Jones and Zimmerman 2010) has been developed based on the Hardy estimates of continuum fields for atomistic systems. The estimation of J-integral for particle-based material point method (MPM) was proposed and the background finite element mesh is used for the calculation (Guo and Nairn 2004). A recent study for the estimation of J-integral using non-local discrete peridynamic formulation (Hu et al. 2012) was developed. The key idea is based on the virtual crack extension concept and a double integral is used to estimate the classical J-integral in the numerical algorithm.

Finite element method (FEM) has an extensive application in the mechanical analysis of the deformation of structures and materials. However, due to the requirement for a fixed topological connectivity between nodes, it always encounters numerical difficulties for the problems with crack, fracture and fragmentation, such as the continuum mesh refinement for a moving crack and the inaccuracies introduced by the highly distorted elements (Belytschko et al. 2013).

So, in recent years, particle-based methods such as VCPM models has attracted

an increasing interests and become a robust alternative to FEM to overcome these difficulties since no re-meshing is necessary (Ostoja-Starzewski 2002; Zhao, Fang, and Zhao 2011; Zhao et al. 2012; G Wang et al. 2009; Ge Wang et al. 2009; Chen, Lin, and Liu 2014). However, due to that large number of particles and small time-steps are usually required in the particle-based methods to guaranty the numerical convergence and stability, particle based method's computational effort is generally much higher than that of FEM (Zhao et al. 2012; G Wang et al. 2009; Ge Wang et al. 2009; Chen, Lin, and Liu 2014). Even though the super computers with parallel technologies can improve the efficiency of methods to some degree, it seems more beneficial to develop a coupling method that can directly bring together the advantages of both methods (Xiao and Belytschko 2004; Fernández-Méndez, Bonet, and Huerta 2005; Zhang, Qiang, and Gao 2011; Liu et al. 2004; Rabczuk, Xiao, and Sauer 2006; Lei and Zang 2010). There are many concurrent methods developed for coupling molecular dynamics models with the continuum models which are very useful in studying local phenomena such as fracture. The region in subdomain modeled by continuum mechanics can be very coarser than in molecular dynamics model and hence, such coupling models permit the use of far less equations than in strict molecular dynamics models.

But, there are some difficulty in such concurrent multiscale coupling models. Doll and Adelman (Doll and Dion 1976; Adelman and Doll 1976) found that, often the high frequency parts of waves are spuriously reflected at the molecular/continuum interface. Holmes and Belytschko (Holmes and Belytschko 1976) also noted the same phenomenon in finite element models with different element sizes. These spurious reflections can be explained by noting that for a wave with a frequency greater than the cutoff frequency of the continuum model, the interface appears as an almost rigid boundary. So instead of smoothly propagating into the continuum model, the high

frequency part of the wave is reflected. This results in spurious growth of energy in the molecular domain.

Recently, several coupling models have been developed. Karpov (Karpov, Wagner, and Liu 2005) developed the coupling methods based on lattice dynamics. He modeled the molecular displacements as the sum of coarse scale and fine scale. A finite element model was used in the continuum model and the spurious reflections at the edge of molecular models are eliminated by introduction of force equivalent to lattice impedance. This included the evaluation of inverse Laplace transforms in time, and for multidimensional problems, a Fourier transform in space. Belytschko and Xiao (Belytschko and Xiao 2003) have developed a coupling method for molecular mechanics and continuum mechanics models based on a bridging domain method. A scaling of the fine and coarse scale potential is used in conjunction with Lagrange multipliers on the overlapping subdomain.

From the above study, here the basic idea is just to use the discrete particle model (VCPM) that can naturally capture the material failures in the regions of interest, e.g. the regions where the fracture process is expected to occur, while use the continuum FEM in the remaining region to reduce the degrees of freedom and improve the simulation efficiencies. Such coupling models are developed using transition elements at the interfaces. (Lin, Chen, and Liu 2015)

There are two major objectives of this study: First, to derive the J-integral using the non-local particle method by (Chen and Liu). The difference of the proposed algorithm with respect to the existing algorithms are: (1) it is not based on the virtual crack extension (Hu et al. 2012) and only need one single integral for the calculation; (2) it is based on the calculation of the particle solutions and does not need the background finite element mesh (Guo and Nairn 2004). And, second, to

develop a seamless particle-FEM coupling method to model the static failure problems in large structures. In the developed coupling method, the dis-continuum domains are described by using the newly developed volume-compensated particle method (VCPM) (Chen, Lin, and Liu 2014) while the continuum domains are modeled by using the traditional finite element method. At the interfaces, virtual VCPM particles are generated and attached to the finite element nodes to account for the non-local effect of VCPM method and to guaranty the interfacial continuity. 10-particle element is also developed to solve the VCPM domains by employing the energy minimization concept shown in the atomic-scale finite element method (AFEM) (Liu et al. 2004). This 10-particle element allows the seamless linkage of VCPM domains with the continuum FEM domains since they are in the same theoretical framework.

Based on the above discussion, the outline of this paper is organized as follows: First, the basic concept and formulations of the VCPM and J-integral is briefly discussed. Next, discussion on the implicit numerical techniques, Atomic Finite Element Method (AFEM), is given for the particle system solution under static loadings. The J-integral estimation is formulated using the particle displacement solutions and stress tensor mapping from the discrete system to its corresponding continuum domain. Following this, the coupling method between the VCPM and FEM is presented in Chapter 2. Then several numerical examples are used in Chapter 3 to validate the proposed algorithm with analytical solutions and finite element solutions, the applications of two coupling methods on the modeling of static fracture problems. Special focus is on the accuracy, convergence, path independence, and failure criterion using the particle-based J-integral estimation. Finally, several conclusions and future work are drawn in Chapter 4 based on the proposed study.

Chapter 2

VOLUMETRIC COMPENSATED PARTICLE MODEL AND COUPLING BETWEEN VCPM AND FEM MODEL

2.1 Brief Review of the Non-local Lattice Particle Method (VCPM)

The proposed J-integral estimation method is based on a non-local lattice particle method called volumetric-compensated particle model (VCPM) (Chen, Lin, and Liu 2014). Detailed derivation can be found in the referred article and only the basic ideas and key equations are reviewed here for the completeness of the description. The basic idea of the VCPM model is to discretize a solid body into particles that are packed in a regular lattice manner and inter-connected by a network of axial springs. In this paper, we only focus on the densest packing of equal-sized spheres, i.e., hexagonal lattice in 2D, as shown in Fig.1(a). The particles at their initial stage are interacting with its neighbors through normal forces, which are represented by normal springs. Thus, a unit cell that periodically repeats the discrete model can be obtained to calculate the strain energy, as shown in Fig.1(b)

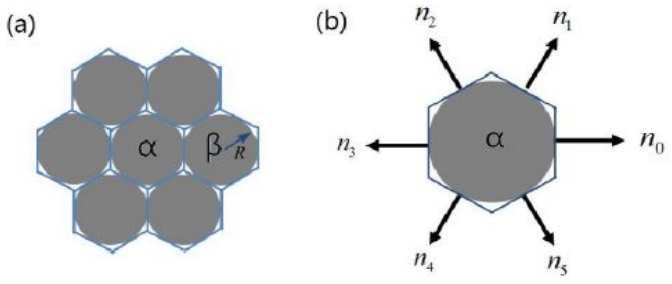

Figure 1. (a) Hexagonal lattice packing of VCPM and (b) Unit cell for hexagonal packing

The strain energy stored in the VCPM unit cell is composed of two parts: the energy stored in the local pair-wise axial springs U_s and the energy associated with the volume change of the particle U_v, which can be expressed as

$$U_{cell} = U_s + U_v \tag{2.1}$$

These energies are given by the following relations:

$$U_s = \frac{k}{2} \sum_{j=1}^{6} (\delta L_{ij})^2 \tag{2.2}$$

$$U_v = \frac{T}{2} \left(\sum_{j=1}^{6} \delta L_{ij}^2 \right) \tag{2.3}$$

where δL is the length change of the entire bond. The model parameters are spring stiffness k and volume change parameter T. These parameters are related to elastic constants (Young's modulus E and Poisson's ratio ν) as,

$$k = \frac{E}{\sqrt{3}(1+\nu)}, T = \frac{\sqrt{3}}{18} \frac{E(4\nu - 1)}{2(1+\nu)(1-2\nu)} \tag{2.4}$$

for the plane strain problems and

$$k = \frac{E}{\sqrt{3}(1+\nu)}, T = \frac{\sqrt{3}}{18} \frac{E(3\nu - 1)(1-\nu)}{2(1-2\nu^2)(1+\nu)} \tag{2.5}$$

for the plane stress problems.

The key factor for the numerical implementation of VCPM model is to accurately define the interaction force between the particles. For an equilibrium system under static / quasi-static loadings, the force acting one each particle must satisfy the equilibrium conditions. The interaction force within a spring given certain length change $\delta l_{\alpha N}$ can be obtained by taking derivative of the total energy of a unit cell U_{cell} with respect to the length change of such spring $\delta l_{\alpha N}$ as:

$$f_{\alpha N} = \frac{\partial U_{cell}}{\partial \delta l_{\alpha N}} \tag{2.6}$$

The final interaction force between particle α and its neighbor particle β can be defined as

$$F_{\alpha\beta} = \frac{1}{2}k_n \delta L_{\alpha\beta} + \frac{\sqrt{3}}{18}T\left(\sum_{N=1}^{6}\delta L_{\alpha N} + \sum_{M=1}^{6}\delta L_{\beta M}\right) \tag{2.7}$$

The particle interaction force consists of two parts: the spring-related part that comes directly from the pair-wise particle interactions and the volume-related part that is associated with the volume changes of those two particles in pair. Since the volume change of a certain particle arises from its connected neighbors, the force between particles is non-local.

Classical particle dynamics can be used to solve the particle systems under loading. Alternatively, energy minimization principle can be used to solve the system implicitly. This algorithm is referred as the Atomic Finite Element Method (AFEM)(Liu et al. 2004).

The energy minimization process can be expressed as

$$\frac{\partial U_{tot}}{\partial x} = 0$$

where $U_{tot} = \sum U_{cell} - \sum_{i=1}^{N} \bar{F}_i \bar{x}_i$ denotes the total energy of the VCPM discrete system; $\bar{F}_i$ is the external force exerted on particle i; $x = (x_1, x_2, ..., x_N)^T$ is the position of particles. The Taylor expansion of U_{tot} around an initial guess $x^{(0)} = \left(x_1^{(0)}, x_2^{(0)}, ..., x_N^{(0)}\right)^T$ of the equilibrium state gives

$$U_{tot} \approx U_{tot}(x^{(0)}) + \frac{\partial U_{tot}}{\partial x}\,|_{x=x^{(0)}}(x - x^{(0)}) + \frac{1}{2}(x - x^{(0)})^T \frac{\partial^2 U_{tot}}{\partial x \partial x}\,|_{x=x^{(0)}}(x - x^{(0)}) \tag{2.8}$$

The following equilibrium equation is obtained:

$$Ku = P \tag{2.9}$$

where $u = x - x^{(0)}$ is the particles' displacement;

$$K = \frac{\partial^2 U_{tot}}{\partial x \partial x}\,|_{x=x^{(0)}} \tag{2.10}$$

is the stiffness matrix;

$$P = (F_i - (\frac{\partial U_{tot}}{\partial x}))\,|_{x=x^{(0)}} \tag{2.11}$$

is the non-equilibrium force vector

It is observed that the governing equation is identical to the governing equation of classical FEM if the particles are taken as nodes. Unlike conventional continuum FEM, we do not divide energy into elements but calculate the first and second order derivatives of Etot needed in the governing equation, directly from this AFEM element. The particle system displacement can be solved using any linear solver, which will be used for the J-integral calculation shown below.

2.1.1 J-integral Estimation Using Particle Displacement Solutions

In this section, we will derive the equation of J-integral for VCPM for a mode I crack. This approach is based on the formulation from Linear Elastic Fracture Mechanics (LEFM). As has been shown by Rice (Rice 1968), the J-integral around a crack tip is path independent. And the expression for calculating the J-integral in 2D case as shown in the figure 2 reads

$$J = -\frac{\partial \pi}{\partial a} = \int_\gamma (w dx_2 - T\frac{\partial u_i}{\partial x_1}) ds \tag{2.12}$$

where, a = crack length, π = potential energy of body, w = strain energy density of a unit cell, T = the traction vector, u_i = displacement vector, ds = a length increment along the contour γ. Equation 2.12 can be rewritten as since $T = \sigma_{ij} n_j$

$$J = \int_\gamma (w n_1 ds - \sigma_{ij} n_j \frac{\partial u_i}{\partial x_1}) ds \tag{2.13}$$

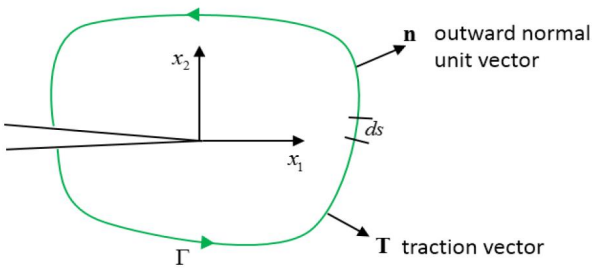

Figure 2. Arbitrary contour around crack tip

$\therefore$

$$J = \int_{\gamma} (w\delta j_1 - \sigma_{ij}\frac{\partial u_i}{\partial x_1})n_j ds \tag{2.14}$$

δj_1 is the components of first column of *kronecker* delta, σ_{ij} is the stress tensor, n_j is the components of the outward normal unit vector.

In order to link the particle system solution to its corresponding continuum domain, the stress tensor mapping is used between these two different formulations. The stress tensor of the unit cell can be obtained through the Cauchy-Born rule (Tadmor, Ortiz, and Phillips 1996). For elastic solids, the strain energy is a function of the strain components only ("Continuum Mechanics for Engineers" 1999),

$$u = u(\epsilon_{ij})$$

$$\dot{u} = \frac{\partial u}{\partial \epsilon_{ij}}\dot{\epsilon}_{ij}$$

so that u is the internal energy. From the energy balance law, we have

$$\dot{u} = \frac{1}{\rho}\sigma_{ij}\dot{\epsilon}_{ij}$$

$$\frac{1}{\rho}\sigma_{ij}\dot{\epsilon}_{ij} = \frac{\partial u}{\partial \epsilon_{ij}}\dot{\epsilon}_{ij}$$

Since $W = \rho u$, one has

$$\sigma_{ij} = \rho\frac{\partial u}{\partial \epsilon_{ij}} = \frac{\partial W}{\partial \epsilon_{ij}}$$

By mapping the stress tensor to the unit cell in the particle system, one can obtain

$$\sigma_{ij} = \frac{\partial W}{\partial \epsilon_{ij}} = \frac{1}{V_{cell}} \frac{\partial U_{cell}}{\partial \epsilon_{ij}} \tag{2.15}$$

The stress tensor at position k can be defined given the strain energy density at the position k as

$$\sigma_{ij}^{(k)} = \frac{1}{A^{(k)}} \frac{\partial U_{particle}^{(k)}}{\partial \epsilon_{ij}^{(k)}} \tag{2.16}$$

where $U^{(k)}$ is the strain energy and $A^{(k)}$ is the corresponding volume at position k. In 2D case, A is the corresponding area.

Using chain rule, Equation 2.16 can be further expanded as

$$\sigma_{ij}^{(k)} = \frac{1}{A^{(k)}} \frac{\partial U_{particle}^{(k)}}{\partial l_{kl}} \frac{\partial l_{kl}}{\partial \epsilon_{ij}^{(k)}} \tag{2.17}$$

where ∂l_{kl} is the spring elongation of the l neighbor of k particle. Applying the strain mapping relationship $e_{kl} = \epsilon_{ij}^{(k)} n_i^{kl} n_j^{kl}$, the stress tensor can be derived as

$$\sigma_{ij}^{(k)} = \frac{l_{kl}}{A^{(k)}} \frac{\partial U_{particle}^{(k)}}{\partial l_{kl}} n_i^{kl} n_j^{kl} \tag{2.18}$$

where n_i^{kl} is unit normal vector for spring kl as shown in Fig. 1(b). If the particle system displacements are solved using the AFEM as described above, Equation 2.14 can be written in the discrete form as

$$J = \sum_{k=1}^{n_\gamma} \left(w^{(k)} \delta j_1 - \sigma_{ij}^{(k)} \frac{\partial u_i^{(k)}}{\partial x_1} \right) n_j^{(k)} \Delta^{(k)} \tag{2.19}$$

where superscript (k) indicates the quantities are evaluated at position k . Thus, J-integral is a contour integral along path γ (see Fig. 2). In the above equation, the derivatives of displacement is required and $(\frac{\partial u_i}{\partial x_1})$ is evaluated using the central difference method.

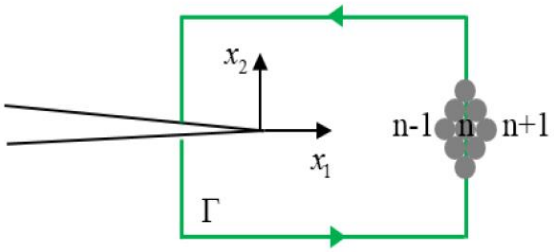

Figure 3. Illustration of central difference scheme

The central difference approximation of $\frac{\partial u_i}{\partial x_1}$ for triangular lattice shown in Figure 3 can be written as:

$$\frac{\partial u_1^{(n)}}{\partial x_1} = \frac{u_1^{-(n+1)} - u_1^{-(n-1)}}{2\Delta x^{(n)}} \tag{2.20}$$

$$\frac{\partial u_2^{(n)}}{\partial x_1} = \frac{u_2^{-(n+1)} - u_2^{-(n-1)}}{2\Delta x^{(n)}} \tag{2.21}$$

where u_i is the components of the displacement vector. Equations 2.19-2.21 are the proposed J-integral estimation formulation.

2.2 Brief Review of Coupling Method

2.2.1 The VCPM Element

As discussed in the previous section, the derivation of VCPM is based on the discrete unit cell energy approximation to the continuum solid. It can be regarded as a very special case of the FEM, where the connectivity of the elements in FEM is reconstructed by a search for the VCPM particle's effective neighbors. When the particle interactions are characterized only by a pair potential, the FEM spring element (linear/nonlinear) can be straightforwardly employed to describe the particle interactions. However, for the VCPM, due to the non-local interactions between the

particle (as shown in equation 2.7), a new VCPM element should be developed to keep the consistency between the VCPM and the FEM and make the coupling between these two methods successful.

In equation 2.7, $\sum_{N=1}^{6} \delta L_{\alpha N}$, are the spring length changes of particle 1's 6 neighbors (spring 1-2, 1-3, 1-4, 1-5, 1-6, 1-7) and $\sum_{M=1}^{6} \delta L_{\beta M}$, are the spring length changes of particle 2's 6 neighbors (spring 2-9, 2-10, 2-3, 2-1, 2-7 and 2-8). We understand that to calculate the spring force between particle α i.e. 1 and particle β i.e. 2, we will need the deformation information of local particles ($\delta L_{\alpha\beta}$ and $\sum_{N=1}^{6} \delta L_{\alpha N}$), and also the deformation information of non-local particles $\sum_{M=1}^{6} \delta L_{\beta M}$. Therefore, totally 10 particle's deformation information will be needed to get the spring force. This is why we design the VCPM element as 10-particle element. The same rule can be applied in the remaining 5 springs for particle.

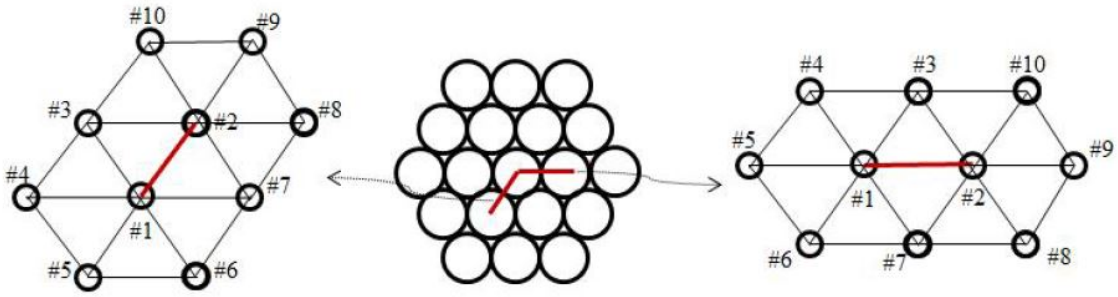

Figure 4. Definition of 10-particle VCPM element according to the particle interaction

A 10-particle VCPM element can be developed as shown in Fig.4. This element consists of two direct interacted particles (particle #1 and particle #2) and their nearest neighbor particles(#2,3,4,5,6,7 for particle #1 and #9,10,3,1,7,8 for particle #2). Such an element captures the non-local effect of the VCPM method, and the internal forces on the two direct interacted particles are calculated according to equation 2.7.

This new element can be applied in the analysis of both dynamic and static problems.

Based on the AFEM method (Liu et al. 2004), K and P can be assembled by the 10-particle VCPM element stiffness matrix $K^{element}$ and the non-equilibrium force vector $P^{element}$, which can be explicitly expressed as:

$$K^{element} = \begin{bmatrix} \left(\frac{\partial^2 U_{\alpha\beta}}{\partial x_1 \partial x_1}\right)_{2\times 2} & \left(\frac{1}{2}\frac{\partial^2 U_{\alpha\beta}}{\partial x_1 \partial x_i}\right)_{2\times 18} \\ \left(\frac{1}{2}\frac{\partial^2 U_{\alpha\beta}}{\partial x_i \partial x_1}\right)_{2\times 18} & (0)_{18\times 18} \end{bmatrix} \tag{2.22}$$

$$P^{element} = \begin{bmatrix} \left(F_1 - \frac{\partial U_{\alpha\beta}}{\partial x_1}\right)_{2\times 1} \\ (0)_{18\times 1} \end{bmatrix} \tag{2.23}$$

Since the above $K^{element}$ and $P^{element}$ for the 10-particle VCPM element are in the same theoretical framework with the conventional FEM element, this provides an opportunity to develop a VCPM/FEM interface linkage to seamlessly couple the two methods

2.2.2 VCPM/FEM Interfacial Coupling Method

Given the above definition of 10-particle VCPM elements, the coupling of VCPM/FEM method conceptually is very similar to the usage of different types of elements in the conventional FEM to solve the whole simulation domain. However, transitional elements should be developed to smoothly link the VCPM and FEM elements, as shown in Fig 5, where the real circle, broken circle, broken hexagon and real rectangle in the figure represent the VCPM particle, the virtual VCPM particle, the effective domain of the VCPM particle and the conventional FEM node, respectively.

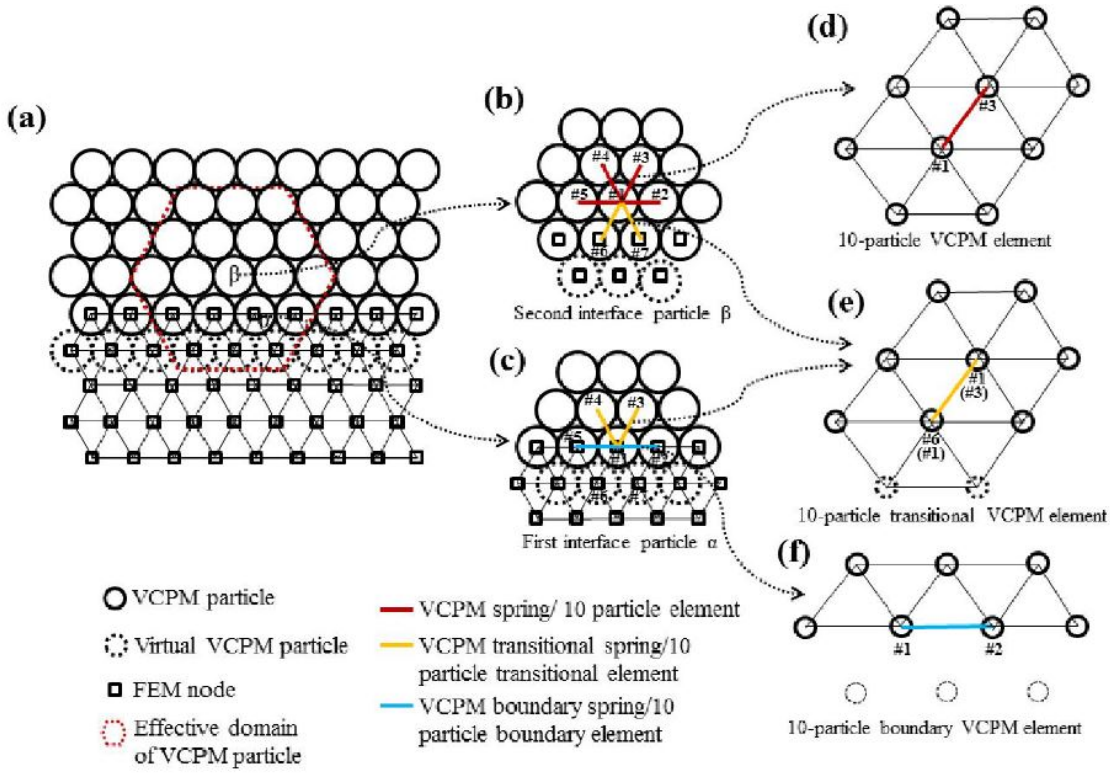

Figure 5. VCPM/FEM edge-to-edge coupling method

(a) virtual VCPM particles attach to the FE nodes; (b) effective domain of second-layer interface particle and the contribution of the six springs to the calculation of forces on the particle; (c) effective domain of first-layer interface particle and the contribution of four springs and three FE elements to the calculation of forces on the particle; (d) 10-particle VCPM element defined on the VCPM springs (spring forces are calculated according to the 10 VCPM particles); (e) 10-particle transitional VCPM element defined on the transitional VCPM springs (spring forces are calculated according to the 8 VCPM particles and 2 virtual particles); (f) 10-particle boundary VCPM element defined on the boundary springs (spring forces are calculated according to the 7 VCPM particles).

Source: Lin, Chen, and Liu (2015)

When coupling two regions, only one layer of virtual VPCM particles are needed (see the dotted circle in Fig.5, they are attached on the FEM nodes). For VCPM particles at the 2^{nd} interface layer, (the particle β in Fig. 5a), one layer of virtual VCPM particles is defined and attached to the FE nodes in order to eliminate the boundary effect and to take count the non-local effect from the FEM domain. As indicated in Fig.5b, the forces exerted on the particle β can be calculated by the derivation of its six neighbor springs' strain energies U_{spring} with respect to the particle's coordination as:

$$F_\beta = \frac{\partial U_{spring}^{1-2}}{\partial x_\beta} + \frac{\partial U_{spring}^{1-3}}{\partial x_\beta} + \frac{\partial U_{spring}^{1-4}}{\partial x_\beta} + \frac{\partial U_{spring}^{1-5}}{\partial x_\beta} + \frac{\partial U_{spring}^{1-6}}{\partial x_\beta} + \frac{\partial U_{spring}^{1-7}}{\partial x_\beta} \tag{2.24}$$

The transitional elements are defined on the spring $\#1-\#6$ and $\#1-\#7$, where the virtual VCPM particles are included to calculate the spring forces. This allows the FE nodes to be added in the particle β 's effective domain, making particle β become equivalent to those bulk particles in the material interiors and avoiding the boundary effect. For VCPM particles at the 1^{st} interface layer (i.e the particle α right at the interface in Fig.5a), the same transition elements as those in the second-layer interfacial particles are defined in the spring #1 - #3 and #1 - #4 to keep the consistency of the springs forces, as shown in Fig. 5c. However, it should be noted that a portion of the deformation energy of the spring #1 - #2 and #1 - #5 have already included in the FE elements $\Delta\#1-\#5-\#6$ and $\Delta\#1-\#7-\#2$. Therefore, the virtual particles are excluded in the definition of the corresponding VCPM elements, and the boundary elements are used in these cases (as indicated in Fig.5f).The forces exerted on the particle α then can be calculated by:

$$F_\alpha = \frac{\partial U_{spring}^{1-2}}{\partial x_\alpha} + \frac{\partial U_{spring}^{1-3}}{\partial x_\alpha} + \frac{\partial U_{spring}^{1-4}}{\partial x_\alpha} + \frac{\partial U_{spring}^{1-5}}{\partial x_\alpha} + \frac{\partial U_{element}^{1-5-6}}{\partial x_\alpha} + \frac{\partial U_{element}^{1-6-7}}{\partial x_\alpha} + \frac{\partial U_{element}^{1-7-2}}{\partial x_\alpha} \tag{2.25}$$

Since the element energies $U_{element}^{1-5-6}$, $U_{element}^{1-6-7}$ and $U_{element}^{1-7-2}$ have significant influence on the calculation of froces on the particle α, the size of the interfacial FEM elements thus is chose to keep the same as the hexagonal packing size of the VCPM particles to reduce the influence and to readily attach the virtual particles to the FE nodes.

The VCPM/FEM coupling method presented above can be readily implemented into the general finite element code since both the VCPM and FEM elements are defined under the same theoretical framework. In fact, we have developed the coupling algorithm in the FORTRAN for the description of VCPM elements.

Chapter 3

NUMERICAL RESULTS AND DISCUSSION

In this section, several numerical studies are done using a single edge cracked rectangular plate model to verify the proposed solution of J-integral. In the numerical simulation, the material parameters are: Young's modulus is 69 GPa and Poisson's ratio is 0.25. The top edge of model is fixed in both the x-direction and y-direction (Fig. 6). The plain strain condition is employed, where pure tensile loading with a displacement of $-5 \times 10^{-4} m$ is applied on the bottom edge of the model as shown in Fig. 6. A sharp edge crack is introduced by breaking the interaction of crack surface particles with its neighbor particles and defining the crack tip as shown in Fig. 6. The proposed simulation results are also compared with the solution from the commercial FEM software ABAQUS. The "seam crack" option is used to create the crack and use special crack tip quadratic elements around the crack tip ("ABAQUS, ABAQUS Theory Manual and Users Manuanl, version62, Hibbit, Karlsson and Sorensen Inc, Pawtucket, RI, USA, 2002." n.d.).

3.1 Stress Response Comparison

Before the comparison of the J-integral, the stress response of the cracked plates are compared first. Traditional methods like point matching entails inferring the stress intensity factor from the stress fields in front of the crack tip (Anderson and Anderson 2005).

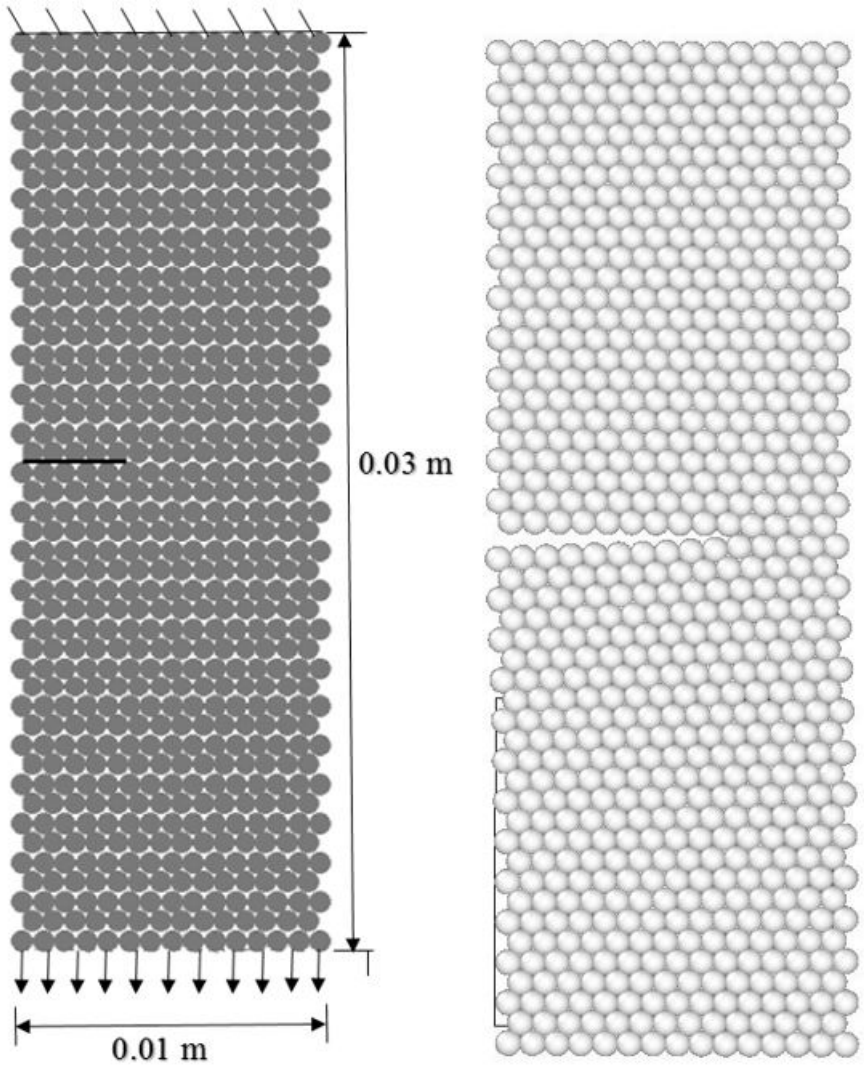

Figure 6. Configuration of a rectangular model and Introduction of sharp crack

On the crack plane ($\theta = 0$), K_I is related to the stress normal to the crack plane as: $K_I = \lim_{r\to\ 0}[\sigma_{yy}\sqrt{2\pi r}]$

The stress-intensity factor can be inferred by plotting the quantity in square brackets against distance from the crack tip, and extrapolating to $r = 0$ as shown in figure 7. It is shown that for plane strain problems, the numerical results are in good agreement with the theoretical values with an error of 7%. If we remove some of

initial particles to obtain the uniform rising slope, the value of K_I converges more to analytical value of FEM as proved from figure 7.

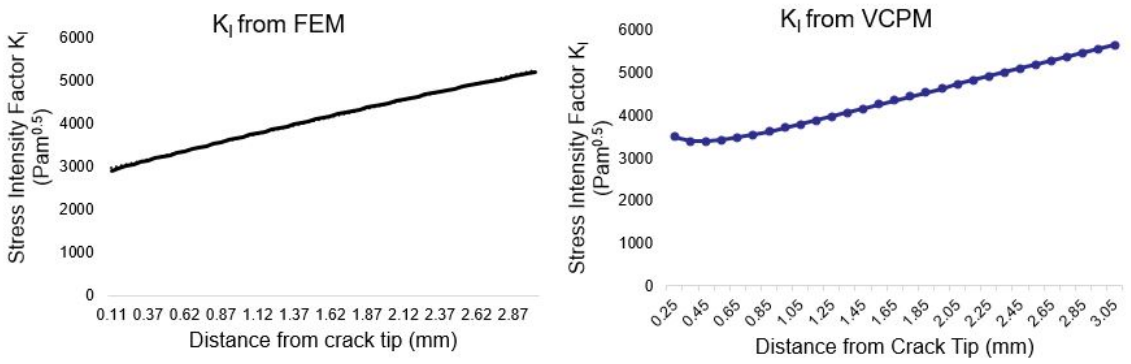

Figure 7. Stress Intensity Factor (K_I) with the distance from crack tip

The stress simulation results predicted by VCPM for the plane strain problems and their comparison with ABAQUS results are shown in Fig. 8. In addition, the stress normal to the crack plane in mode I is plotted and compared with the same from ABAQUS results as given in Fig. 8. It is observed that the VCPM has almost the identical stress distribution with that from the classical FEM in ABAQUS.

Since the J-integral involves the components of stress and displacement fields, it is of interest to compare these fields with those obtained from sufficiently fine classical FEM mesh. As shown in Fig 9 and Fig 10, the contour plots of stress field in x and y-directions are almost identical to the FEM calculations. This comparison verifies the proposed finite element implementation of VCPM J integral. Since the mesh sizes are different in both systems and one is of particle nature, somewhat non-uniform contours may be seen.

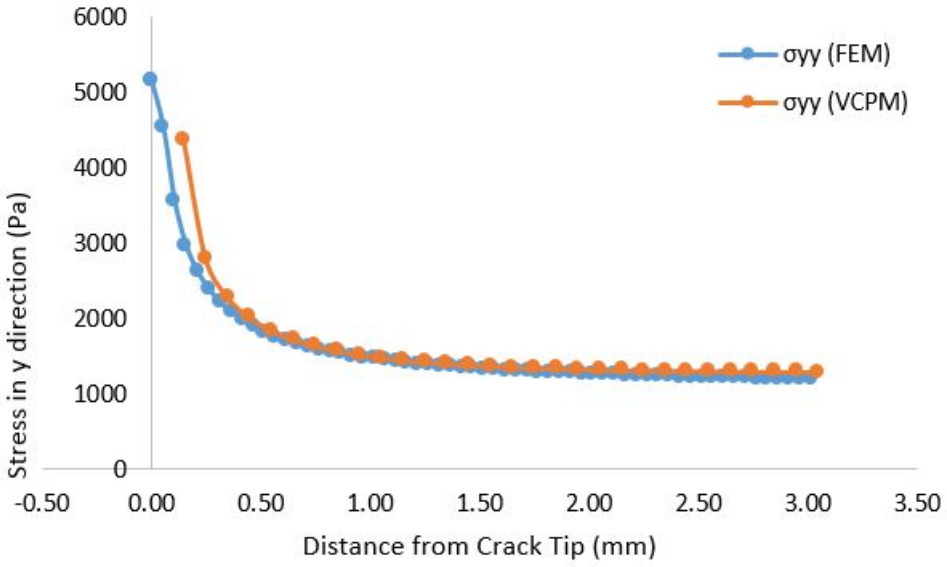

Figure 8. Comparison of stress fields in y-direction in front of the crack tip

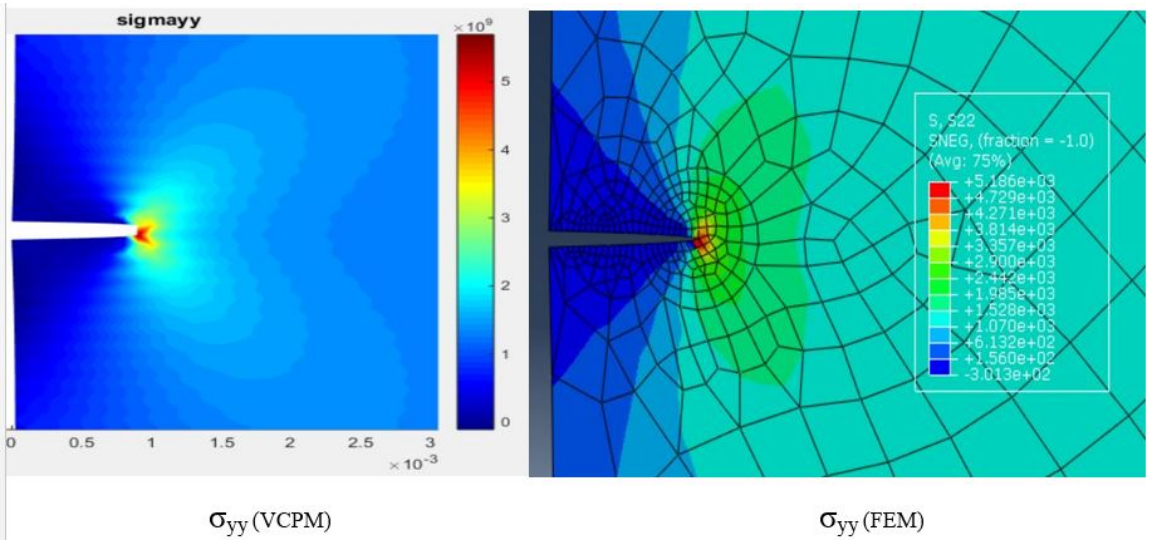

Figure 9. Contour plots of stress in y-direction obtained by VCPM and FEM

3.2 Convergence Study

The convergence characteristic of the VCPM model is simulated with different particle sizes by using the same simulation model and the results are summarized in

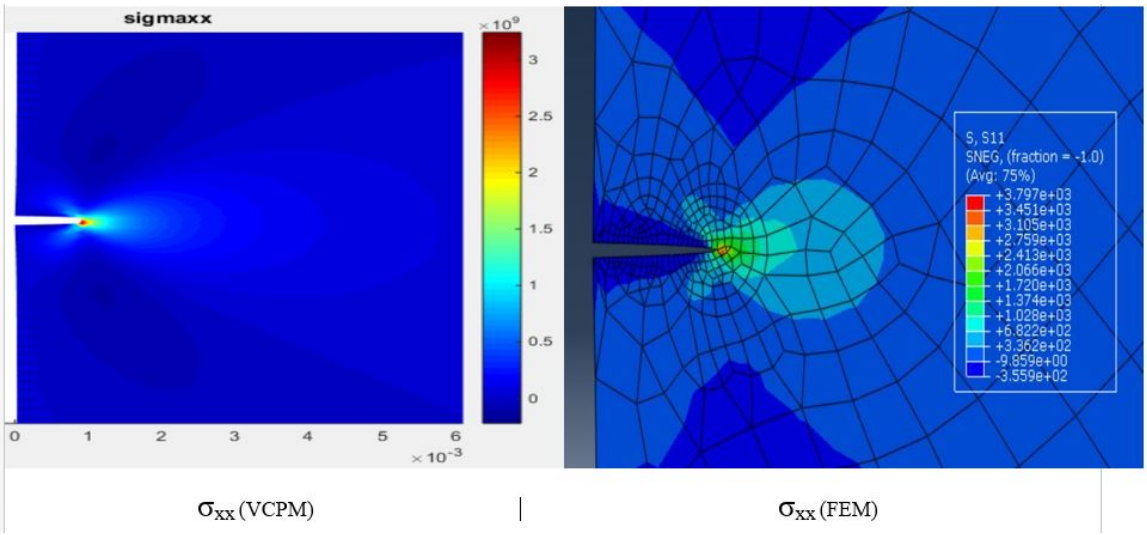

Figure 10. Contour plots of stress in x-direction obtained by VCPM and FEM

Table 1 and Figure 11. As can be seen from figure, the value of J-integral converges as the number of particles increases. Unlike the classical FEM method, the convergence for the particle-based J-integral is partially due to the "skin-effect" in the discrete formulation. The particles at the free edge do not have their complete neighbors as the unit cell. Thus, if the particle number is small, the impact of the free edge particle to the entire simulation domain is higher. In the proposed study, no intent to correct the "skin-effect" is made and it is required additional investigations. The proposed study increase the total particle numbers and the percentage of free edge particles reduces and their effect also reduces. Thus, in the following analysis, in order to make a better comparison with FEM results, the particle radius $R = 5 \times 10^{-5}$m (total number of particles of model is 34874) is used as the convergence study indicates that this is sufficient for the J-integral estimation

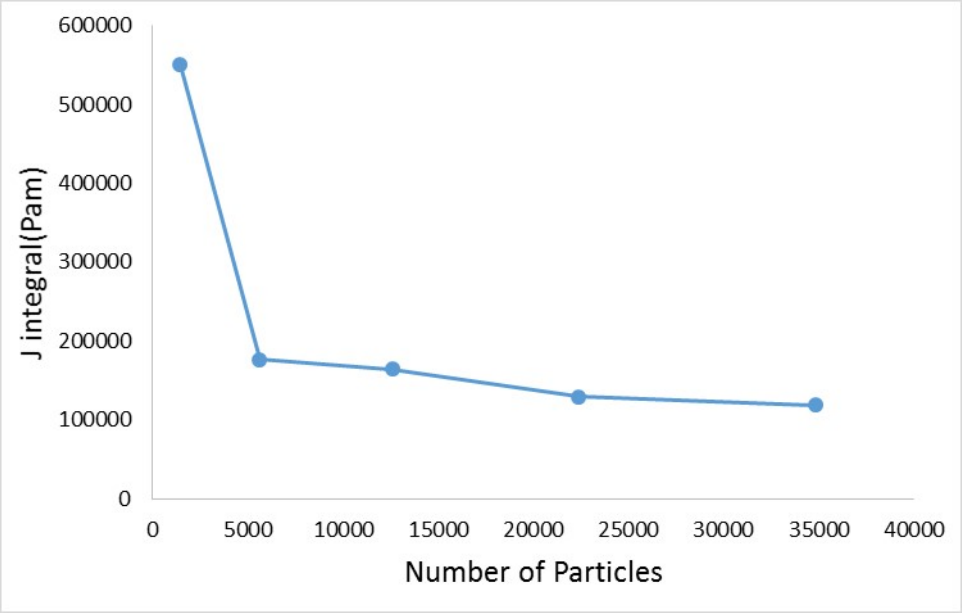

Figure 11. Convergence of J-integral with particle density

Table 1. Convergence of J-integral with particle density

Number of Particles on model's bottom edge	21	41	61	81	101
Total number of particles	1435	5630	12584	22379	34874
Particle Radius (m)	2.5×10^{-4}	1.25×10^{-4}	8.33×10^{-5}	6.25×10^{-5}	5×10^{-5}
J-integral (Pam)	549824	176905	164239	129804	118572
Error(%)	364	49.57	38.86	9.75	0.25

3.3 Path Independence of the Proposed J-integral Calculation Algorithm

Rice (Anderson and Anderson 2005) presented a mathematical proof of the path independence for the J-integral. The proposed particle-based J-integral estimation algorithm should also have this property and is verified here. Four different contours are used for the J-integral calculation and the schematic plot is shown in Fig. 12. Contour (a) is close to crack tip and contour (d) is away from the crack tip. The values are given in table 2. The errors for the J-integral estimation is calculated by

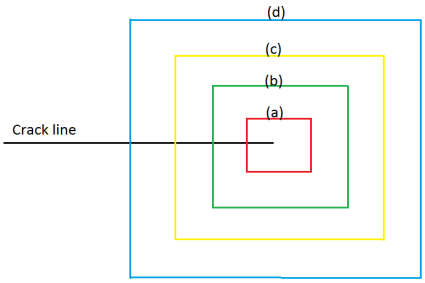

Figure 12. Four different integral contours to compute VCPM J integral

assuming the ABAQUS results as the ground truth. The errors are normalized using the ABAQUS results and are shown in table 2. It is shown that the path independence for the proposed J-integral estimation is valid.

Table 2. Path independence of J-integral

	Contour a	Contour b	Contour c	Contour d
J integral(Pam)	124793	118572	116012	112847
Error (%)	5.53%	0.27%	1.88%	4.56%

3.4 Accuracy Study

In this section, the accuracy of the proposed J-integral estimation is investigated by comparing the solutions with that from the ABAQUS for various crack lengths. Due to the finite dimension of the plate, the geometric correction for the finite dimension will affect the final J-integral estimation. Results of the proposed J-integral calculation for VCPM and coupling model and ABAQUS solution are shown in figure 13. Satisfactory results are observed for different crack lengths. It is seen that the error increases as the crack length increases. This is probably due to the "skin effect" since the contour will be close to the free surface boundary when the crack lengths increases. Table 3

shows the percentage error in J-integral of VCPM and coupling model compared with ABAQUS FEM model.

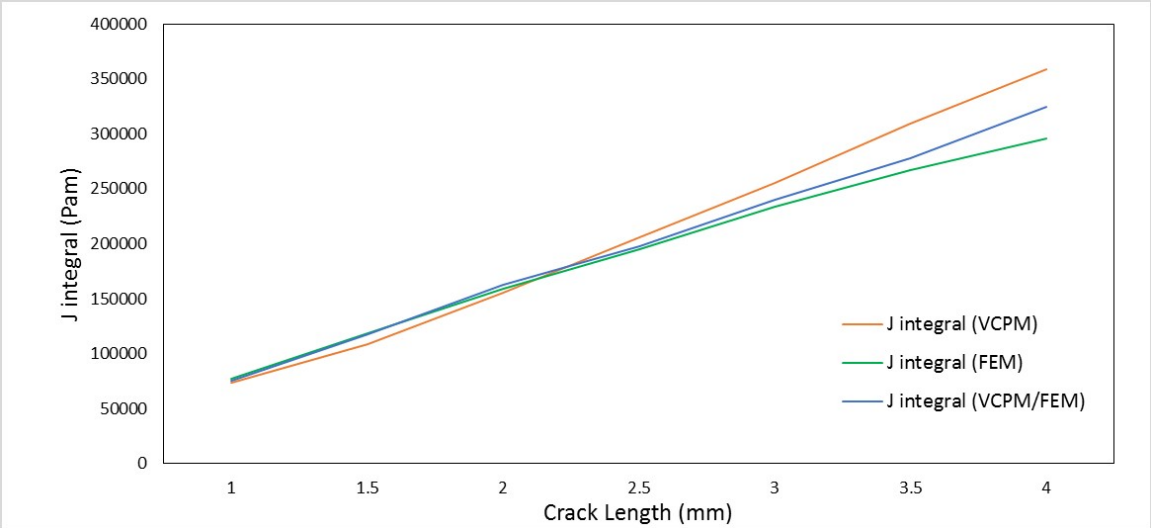

Figure 13. J-integral versus crack length in mode I

Table 3. Error in J-integral of VCPM and Coupling model compared with FEM model

Crack Length (mm)	1	1.5	2	2.5	3	3.5	4
VCPM	4.03%	8.01%	2.09%	5.25%	9.3%	15.93%	21.36%
VCPM/FEM	1.45%	0.64%	2.47%	1.4%	2.58%	4.01%	8.9%

3.5 VCPM/FEM Coupling Model Results

The geometry dimensions and boundary conditions of the static beam problem are similar to the beam explained earlier just the beams center region is discretized by VCPM particles as shown in Fig.14 . The material properties are set as $E = 69$ GPa and $\nu = 0.25$. The upper edge of beam is fixed in x and y directions and a uniform displacement field of -5×10^{-4} (tensile load) is applied on bottom edge.

The VCPM/FEM coupling simulation results are firstly compared with those of FEM and pure VCPM to verify the proposed method, as shown in Fig.17. The Uy displacements along the center line of the beam are plotted in figure.

To allow a better comparison, the nodes in the FEM model and the particles/nodes in the VCPM/FEM model are kept at the same coordinates. Also the continuity of the displacement across the VCPM and FEM interface can be observed through the introduction of transition elements as shown in fig.15. The figure shows the displacement contour plots along the top and bottom coupling interface.

The continuity of the displacement across the VCPM/FEM coupling interface can also be seen in Fig.16, which shows the displacements along the beam's bottom and top coupling interface, respectively.

3.5.1 J integral in VCPM/FEM Coupling Model

Since the J integral is already formulated and calculated for VCPM model, it is of great interest to estimate the J integral value in VCPM/FEM coupling model which proves the feasibility of the proposed algorithm. The same contour integral methodology as used above is adopted in the particle region to find J value. For different crack lengths, the value of J-integral from coupling model is estimated and compared with those of pure VCPM and FEM model. The figure 13 and table 3 shows the variation of J-integral with crack lengths and error with FEM model respectively.

Hence, it can be concluded that with the same formulation of J integral in VCPM model, J integral in VCPM/FEM coupling model also can be accurately estimated.

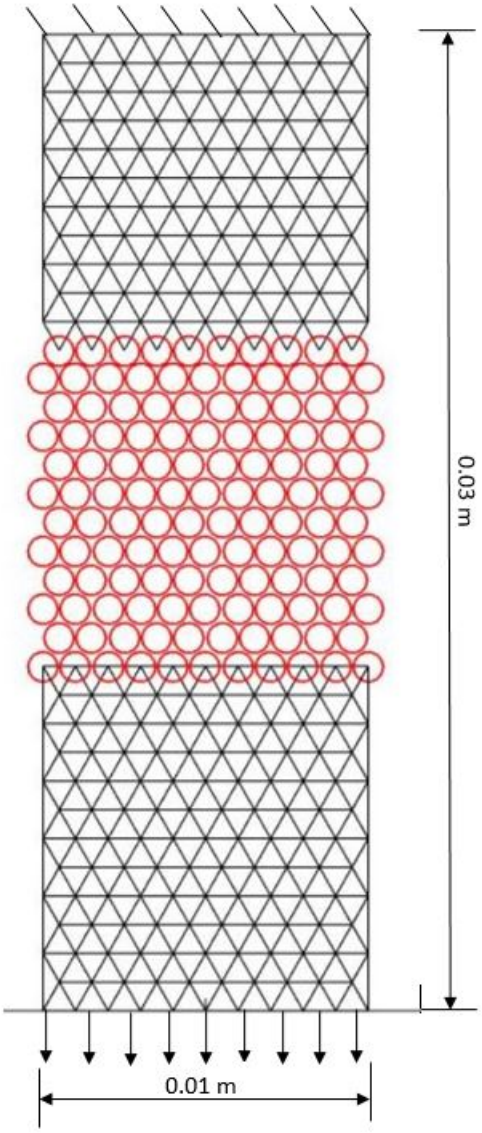

Figure 14. The geometry of VCPM/FEM coupling model

3.5.2 Static Crack Growth Simulation using Fracture Criterion

Extensive researches have been proposed to simulate crack initialization, propagation, branching from different engineering discipline. The developed numerical methods can be categorized into two groups: the continuum-based methods and the

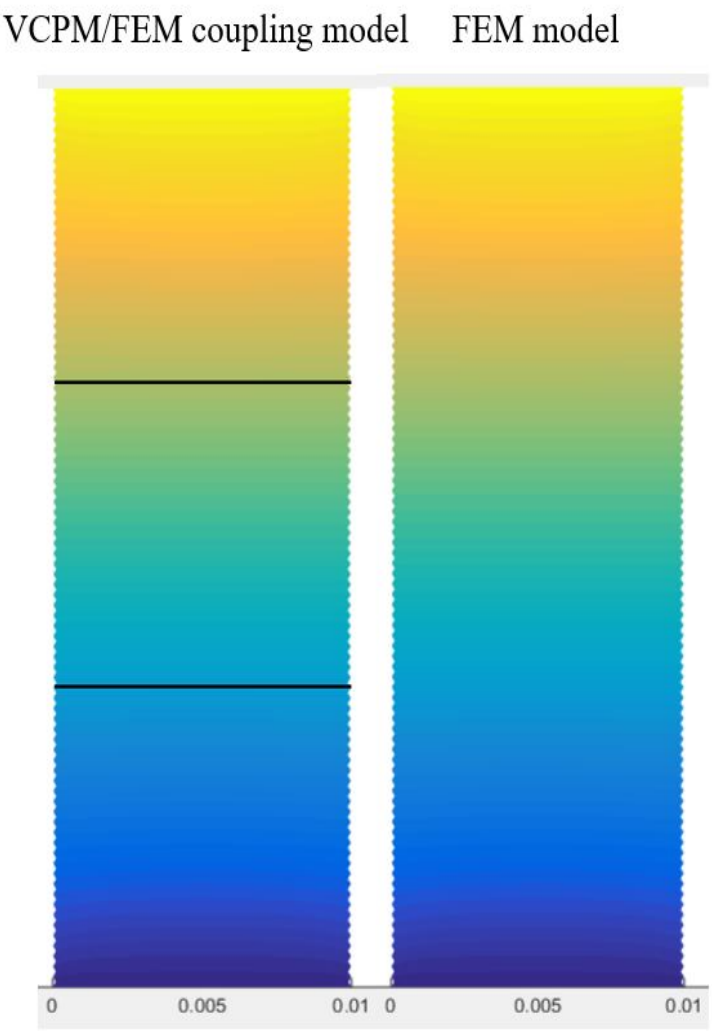

Figure 15. Uy displacement field for VCMP/FEM coulping model and FEM model

discontinuous approaches. For fracture problems, the classical finite element method (FEM) uses mesh matching and remeshing techniques which is computationally very expensive. The cohesive elements does not require very dense mesh near the crack tip region, but usually requires the crack path as a prior knowledge for the computational efficiency. eXtended FEM (XFEM) treats the discontinuity via level sets method and enrich the crack tip elements with analytical solution for the stress or displacement from linear elastic fracture mechanics. Arbitrary crack branching and coalesce is still

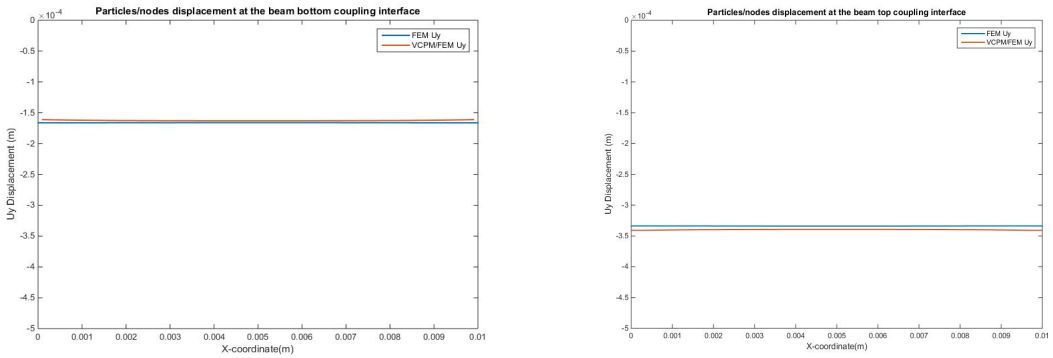

Figure 16. Particles/nodes displacement at the beam's bottom and top coupling interface

challenging in the XFEM framework. The discontinuous approaches, such as lattice particle models and peridynamics, can handle fracture problems very efficiently. No additional criteria are needed as the crack growth is a natural outcome of the system evolution. As the elongation of the connecting bonds exceeds the critical value, it breaks and the crack propagates automatically.

Interfacial debonding in above beam specimen using a dedicated VCPM region near crack tip is tested first. The simple bond based critical force failure criterion is adopted to demonstrate the capability of fracture modeling. Thus, the spring breaks when,

$$F_n \geq F_c \tag{3.1}$$

where F_n is the normal force and F_c is the critical normal force defined by the failure criteria. Within the linear elastic fracture mechanics, for a given material, the above critical force criterion can be derived from the material strength through $F_c = 2R\sigma_s/\sqrt{3}$ (where R is the particle radius). And it can also be readily related to the critical energy/ elongation criterion based on the material properties, such as the fracture toughness $K_{Ic} = Y\sigma_s\sqrt{\pi a}$ (where a is the initial crack length) and the critical energy release rate $G_{Ic} \approx K_{Ic}^2$.

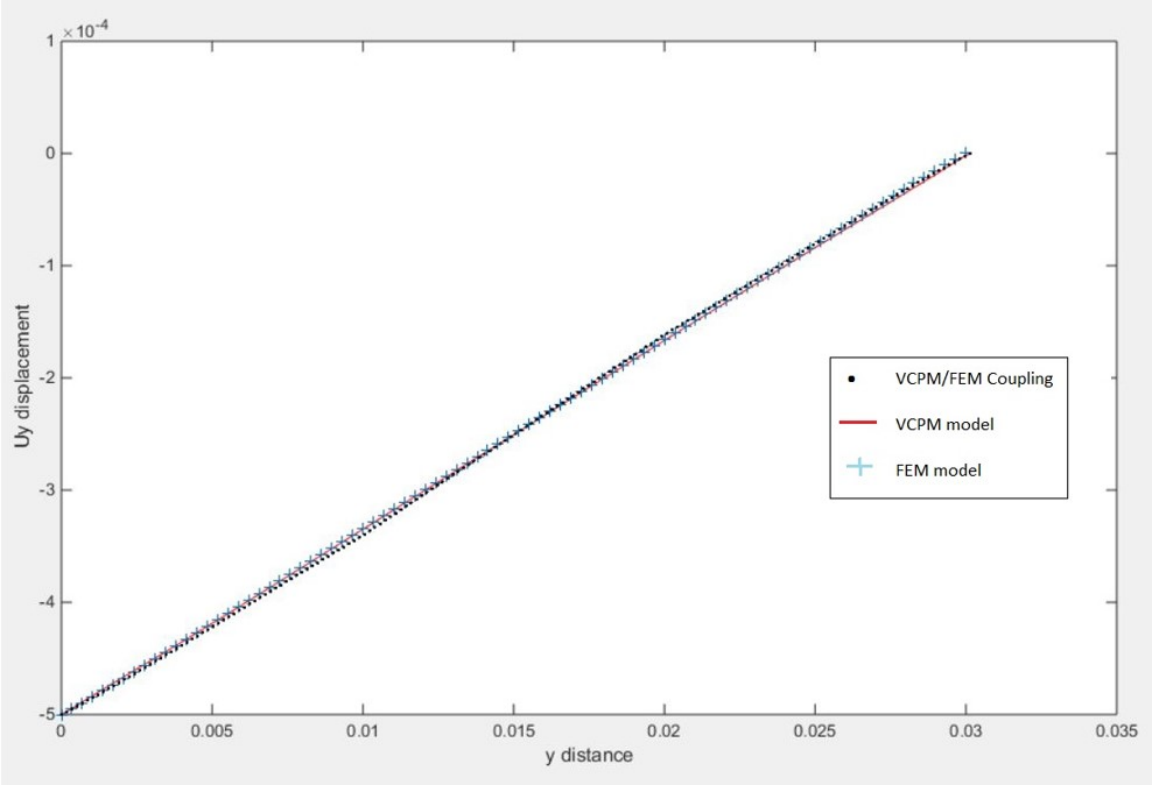

Figure 17. Comparison of VCPM/FEM simulation results with those of FEM and VCPM model: Particles/nodes displacements along the center line of the beam

During the simulation, the system's equilibrium states are evaluated according in each iteration step and the corresponding spring forces are calculated according to equation 2.7. Whenever the force of an equilibrated spring exceeds the critical one in equation 3.1, it is deleted and excluded in the following iteration steps. When the location of crack tip exceeds the boundaries of particle domain, particle domain is shifted ahead to accurately capture the crack effects.

In the current simulation, the material parameters of model are set as $E = 69$ GPa and $\nu = 0.25$ with particle radius $R = 1 \times 10^{-4}m$; the springs' critical force is set as $F_c = 54272N$; and the force increment is chosen as 1×10^{-4}. The crack growth

at different loading stages are shown in Fig.18 The section is zoomed to accurately view the particle region.

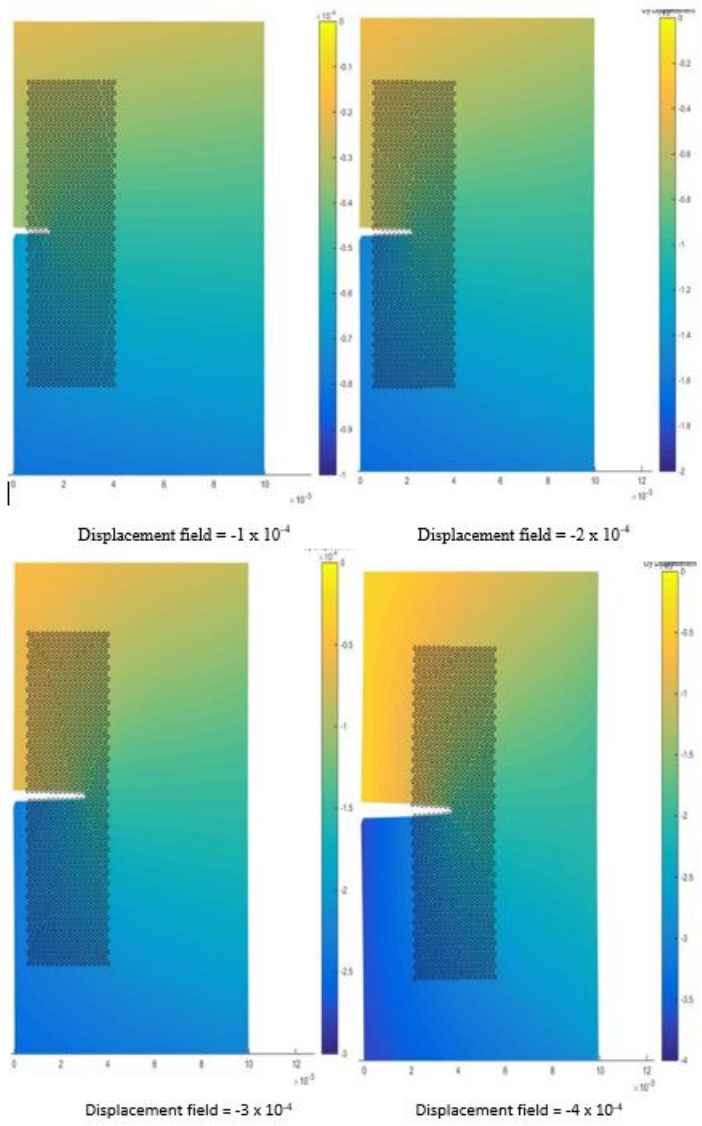

Figure 18. The static crack propagation predicted by VCPM/FEM coupling model at different loading stages. The pictures are colored according to the u_y displacement.

3.5.3 Maximum Force as a Material Property

The maximum force developed in the particle spring in front of the crack tip can be estimated using the equation 2.7. To prove that maximum force developed in the spring is a material property, the maximum force for different number of particles i.e. different mesh sizes is plotted as shown in Fig. 19.

From the curve, it can be inferred that as the particle numbers increases, the curve converges to a constant value. It means that the maximum force if treated as a critical force parameter, can be concluded that it is a material property . Since critical force can be readily related to the critical energy/ elongation criterion based on the material properties and can be easily derived from a material strength. This behavior is unlike in classical FEM where the plot of maximum stress developed in front of the crack tip with element size/mesh density, increases continuously.

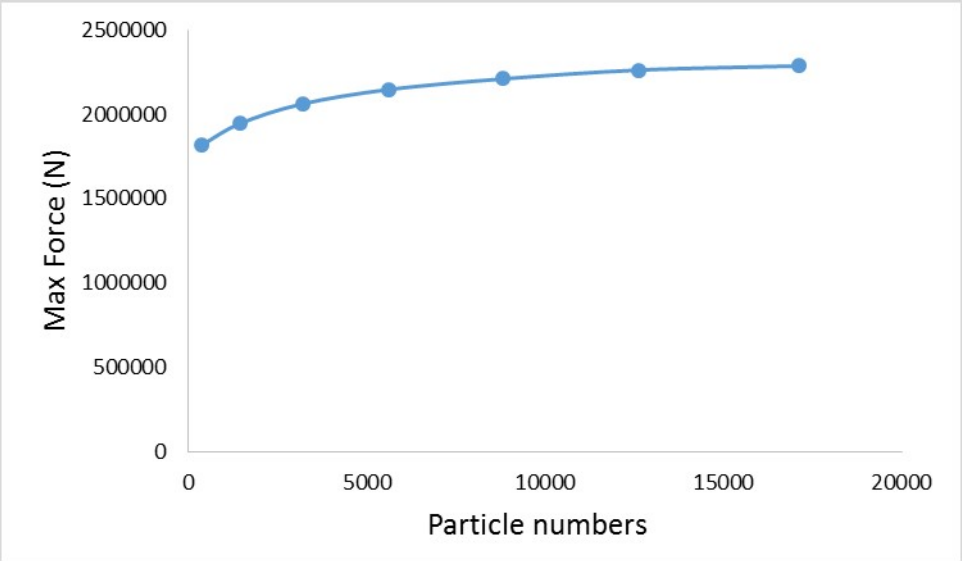

Figure 19. Maximum force as a material property

Chapter 4

CONCLUSION AND FUTURE WORK

A new non-local particle method-based J-integral estimation algorithm is proposed in this paper and verified with classical finite element results. The coupling algorithm is also developed between non-local particle model and classical FEM model. In the developed coupling method, the VCPM model is implemented in the regions of interests such as crack initiation and propagation. Several conclusions can be drawn based on the current investigation-

- The proposed J-integral does not need continuum-based finite element mesh for the calculation of the contour integral and can be directly calculated using the particle system solution, which avoid the interpolation using shape function in classical FEM. It is noted that the used atomic finite element method does not involve any approximations like shape functions since it uses only the first and second order derivatives of particle's strain energy.

- The calculated J-integral is non-local as compared to the classical J-integral since the traction force on the contour depends on the non-local particle displacement in the proposed particle-based algorithms. The calculated values are same compared with the FEM-based calculation and also shows that path-independence of the classical J-integral.

- The intrinsic "skin-effect" of the discrete formulations affects the computational efficiency of the J-integral estimation, especially when the contour is close to the free surfaces. Future study is required to improve this behavior and the proposed study

suggest two tentative ways to reduce the "skin effect": increase of particle density and contour selection should be away from the free surfaces.

- The proposed coupling method is applied in the static beam simulation to find the J integral. The calculated values for different crack lengths are witinn a range compared to the FEM based calculation which indicate that the coupling method works well and also maintains the computational accuracy.

- The static crack growth simulation is performed using coupling algorithm through simple bond based critical force failure criterion. Unlike classical FEM static simulation where critical energy release rate criteria is used, coupling model uses simple bond based critical force failure criterion which is easy and simple to implement.

- The current investigation is only for linear elastic analysis. Additional study is required for J-integral calculation for nonlinear plastic materials. Additional investigation is required for the "skin effect" in the particle-based J-integral calculations. The calculation and application of J-integral for growing crack needs more effort

- More investigation needs to be performed on coupling model. The classical FEM mesh needs to be of varying size i.e. coarse far from region of interest and gradually getting denser near the interest region. This will greatly reduce the computer efforts.

REFERENCES

"ABAQUS, ABAQUS Theory Manual and Users Manuanl, version62, Hibbit, Karlsson and Sorensen Inc, Pawtucket, RI, USA, 2002." n.d.

Adelman, SA, and JD Doll. 1976. "Generalized Langevin equation approach for atom/solid-surface scattering: General formulation for classical scattering off harmonic solids." *The Journal of chemical physics* 64 (6): 2375–2388.

Anderson, Ted L, and TL Anderson. 2005. *Fracture mechanics: fundamentals and applications.* CRC press.

Belytschko, Ted, Wing Kam Liu, Brian Moran, and Khalil Elkhodary. 2013. *Nonlinear finite elements for continua and structures.* John Wiley & Sons.

Belytschko, Ted, and SP Xiao. 2003. "Coupling methods for continuum model with molecular model." *International Journal for Multiscale Computational Engineering* 1 (1).

Chen, Hailong, Enqiang Lin, and Yongming Liu. 2014. "A novel Volume-Compensated Particle method for 2D elasticity and plasticity analysis." *International Journal of Solids and Structures* 51 (9): 1819–1833.

"Continuum Mechanics for Engineers." 1999. In *Continuum Mechanics for Engineers, Second Edition.* Computational Mechanics and Applied Analysis. CRC Press, June. doi:doi:10.1201/9781439832578.fmatt.

Doll, JD, and DR Dion. 1976. "Generalized langevin equation approach for atom/solid–surface scattering: Numerical techniques for gaussian generalized langevin dynamics." *The Journal of Chemical Physics* 65 (9): 3762–3766.

Fernández-Méndez, Sonia, Javier Bonet, and Antonio Huerta. 2005. "Continuous blending of SPH with finite elements." *Computers & structures* 83 (17): 1448–1458.

Gao, Huajian, and Patrick Klein. 1998. "Numerical simulation of crack growth in an isotropic solid with randomized internal cohesive bonds." *Journal of the Mechanics and Physics of Solids* 46 (2): 187–218.

Guo, Yajun, and John A Nairn. 2004. "Calculation of J-integral and stress intensity factors using the material point method." *Computer Modeling in Engineering and Sciences* 6:295–308.

Holian, Brad L, and Ramon Ravelo. 1995. "Fracture simulation using large-scale molecular dynamics." *Phys.\ Rev.˜ B* 51 (17): 275–288.

Holmes, N, and T Belytschko. 1976. "Postprocessing of finite element transient response calculations by digital filters." *Computers & Structures* 6 (3): 211–216.

Hrennikoff, Alexander. 1941. "Solution of problems of elasticity by the framework method." *Journal of applied mechanics* 8 (4): 169–175.

Hu, Wenke, Youn Doh Ha, Florin Bobaru, and Stewart A Silling. 2012. "The formulation and computation of the nonlocal J-integral in bond-based peridynamics." *International journal of fracture* 176 (2): 195–206.

Jin, Y, and FG Yuan. 2005. "Atomistic simulations of J-integral in 2D graphene nanosystems." *Journal of nanoscience and nanotechnology* 5 (12): 2099–2107.

Jones, Reese E, and Jonathan A Zimmerman. 2010. "The construction and application of an atomistic J-integral via Hardy estimates of continuum fields." *Journal of the Mechanics and Physics of Solids* 58 (9): 1318–1337.

Karpov, EG, GJ Wagner, and Wing Kam Liu. 2005. "A Green's function approach to deriving non-reflecting boundary conditions in molecular dynamics simulations." *International Journal for Numerical Methods in Engineering* 62 (9): 1250–1262.

Lei, Zhou, and Mengyan Zang. 2010. "An approach to combining 3D discrete and finite element methods based on penalty function method." *Computational Mechanics* 46 (4): 609–619.

Lin, Enqiang, Hailong Chen, and Yongming Liu. 2015. "Coupling between non-local particle and finite element methods." In *Proceedings of AIAA Modeling and Simulation Technologies Conference.* American Institute of Aeronautics and Astronautics.

Liu, B, Y Huang, H Jiang, S Qu, and KC Hwang. 2004. "The atomic-scale finite element method." *Computer methods in applied mechanics and engineering* 193 (17): 1849–1864.

Noor, Ahmed K. 1988. "Continuum modeling for repetitive lattice structures." *Applied Mechanics Reviews* 41 (7): 285–296.

Ostoja-Starzewski, Martin. 2002. "Lattice models in micromechanics." *Applied Mechanics Reviews* 55 (1): 35–60.

Rabczuk, Timon, Shao Ping Xiao, and M Sauer. 2006. "Coupling of mesh-free methods with finite elements: basic concepts and test results." *Communications in Numerical Methods in Engineering* 22 (10): 1031–1065.

Rice, James R. 1968. "A path independent integral and the approximate analysis of strain concentration by notches and cracks." *Journal of applied mechanics* 35 (2): 379–386.

Tadmor, Ellad B, Michael Ortiz, and Rob Phillips. 1996. "Quasicontinuum analysis of defects in solids." *Philosophical Magazine A* 73 (6): 1529–1563.

Wang, G, A Al-Ostaz, AH-D Cheng, and PR Mantena. 2009. "A macroscopic-level hybrid lattice particle modeling of mode-I crack propagation in inelastic materials with varying ductility." *International Journal of Solids and Structures* 46 (22): 4054–4063.

Wang, Ge, A Al-Ostaz, AH-D Cheng, and PR Mantena. 2009. "Hybrid lattice particle modeling: theoretical considerations for a 2D elastic spring network for dynamic fracture simulations." *Computational Materials Science* 44 (4): 1126–1134.

Xiao, SP, and Ted Belytschko. 2004. "A bridging domain method for coupling continua with molecular dynamics." *Computer methods in applied mechanics and engineering* 193 (17): 1645–1669.

Zhang, Zhichun, Hongfu Qiang, and Weiran Gao. 2011. "Coupling of smoothed particle hydrodynamics and finite element method for impact dynamics simulation." *Engineering Structures* 33 (1): 255–264.

Zhao, Gao-Feng, Jiannong Fang, and Jian Zhao. 2011. "A 3D distinct lattice spring model for elasticity and dynamic failure." *International Journal for Numerical and Analytical Methods in Geomechanics* 35 (8): 859–885.

Zhao, Gao-Feng, Nasser Khalili, Jiannong Fang, and Jian Zhao. 2012. "A coupled distinct lattice spring model for rock failure under dynamic loads." *Computers and Geotechnics* 42:1–20.

Zimmerman, Jonathan A, and Reese E Jones. 2013. "The application of an atomistic J-integral to a ductile crack." *Journal of Physics: Condensed Matter* 25 (15): 155402.